Transient Analysis of a Circular Foil Gage in a Convective and Radiative Environment[1]

Jiann C. Yang[2]

Fire Research Division
Engineering Laboratory
National Institute of Standards and Technology
Gaithersburg, MD 20899, U.S.A.

ABSTRACT

An analysis of a circular thin-foil gage is presented that includes transient effects, convective heat transfer, and an arbitrary time-varying boundary condition at the foil edge to account for fluctuations in cooling water temperature. The governing energy equation is solved using Laplace transform to obtain the temporal and spatial temperature distributions of the foil. Under constant temperature at the foil edge and constant thermal radiative heat flux, closed-form response curves for the gage under various modes of heat transfer are provided. Steady-state results are also presented as limiting cases.

Keywords: Heat conduction; heat convection, heat flux gage; thermal radiation

Introduction

In 1953, Gardon [1] developed a circular thin-foil gage to measure thermal radiation and provided a simple steady state heat conduction analysis to describe the operation of the gage. Since then circular thin-foil gages, sometimes referred to as Gardon gages named in honor of Gardon, have been used extensively in fire research and testing [2], solar radiation measurements [3], and other aerospace applications [4]. A cross section of the gage is depicted in Figure 1. The gage sensing element is made from constantan metal foil in the form of a circular disk and is attached to a water-cooled constant-temperature copper ring. When the incident heat flux strikes the foil, the energy absorbed by the foil diffuses radially toward the outer circumference of the foil and into the copper ring acting as a heat sink, causing a temperature difference between the foil center and the edge. The temperature difference, which is measured using a differential thermocouple, can be related to the incident heat flux.

Analytical studies have been reported in the literature to examine various aspects of the thin-foil gage operation and performance. Gardon [1] originally modeled the gage by treating it as a one-dimensional steady-state heat conduction through the foil in the radial direction to obtain the temperature distribution in the foil with an applied uniform thermal radiative heat flux on the foil. Malone [4] used a one dimensional steady-state formulation to analyze convective heat transfer to or from a radiantly heated foil and heat loss down the center wire. Ash [5] studied the transient response characteristics of thin-foil heat flux sensors under thermal radiative or convective environment. Kirchoff [6] provided a two-dimensional transient heat conduction analysis on the foil to study the effect of foil thickness on the gage response without considering

heat convection. A one-dimensional transient heat conduction model was developed by Keltner and Wildin [7] to examine transient response of the gages. Borell and Diller [8], Kuo and Kulkarni [9], and Fu et al. [10] expanded the steady-state analysis of Gardon [1] by including convective heat transfer at the foil surface and provided calibration corrections for convective heat transfer. Recently, Fu et al. [11] applied the Duhamel theorem to study Gardon gage exposed to fast heat flux transients.

Here the analysis is expanded to include transient effects, convective heat transfer, and the time-varying heat-sink temperature to reflect fluctuations in cooling water temperature. However, we still limit our analysis to one dimension in the radial direction of the foil exposed to a constant radiative heat flux.

Formulation and Analysis

Assuming no heat conduction loss along the copper wire at the center of the foil, no convective heat transfer on the backside of the gage, and constant thermophysical properties of the foil, the energy equation for the foil is

$$\frac{\partial^2 T}{\partial r^2} + \frac{1}{r}\frac{\partial T}{\partial r} + \frac{q_i}{kH} + \frac{h}{kH}(T_\infty - T) = \frac{1}{\alpha}\frac{\partial T}{\partial t} \tag{1}$$

with the following initial and boundary conditions

I.C.: at $t = 0$, $T = T_0$ for $0 \le r \le R$

B.C. 1: at $r = 0$, $\partial T / \partial r = 0$ or T is finite

B.C. 2: at $r = R$ $T = f(t)$

The boundary condition (B.C. 2) at $r = R$ reflects an arbitrary time-varying heat-sink temperature.

Introducing the following dimensionless variables:

$\xi = r/R$ $\tau = \alpha t / R^2$ $\theta = T/T_0$

With $Nu = hR/k_f$, $Q^* = q_i R^2 / kHT_0$, $\kappa = k_f/k$, $\delta = R/H$, and $Nu^* = \kappa\delta Nu$, Eq. (1) can be non-dimensionalized to

$$\frac{\partial^2 \theta}{\partial \xi^2} + \frac{1}{\xi}\frac{\partial \theta}{\partial \xi} - Nu^* \theta + (Q^* + Nu^* \theta_\infty) = \frac{\partial \theta}{\partial \tau} \tag{2}$$

I.C.: at $\tau = 0$, $\theta = \theta_0$ for $0 \le \xi \le 1$

B.C. 1: at $\xi = 0$, $\partial \theta / \partial \xi = 0$

B.C. 2:   at $\xi = 1$ $\theta = \theta_f(\tau) = f(\tau)/T_0$

Equation (2), together with the non-dimensionalized initial and boundary conditions, can be solved using Laplace transform. In the following, the Laplace transform and its inverse transform operators are represented by L and L^{-1} respectively, and we use $\hat{\theta}(\xi, s)$ to denote the transformed variable of $\theta(\xi, \tau)$ with respect to τ.

Taking Laplace transform of Eq. (2) with respect to τ,

$$L\left\{\frac{\partial^2\theta}{\partial\xi^2} + \frac{1}{\xi}\frac{\partial\theta}{\partial\xi} - Nu^*\theta + (Q^* + Nu^*\theta_\infty)\right\} = L\left\{\frac{\partial\theta}{\partial\tau}\right\}$$

$$\frac{\partial^2\hat{\theta}(\xi,s)}{\partial\xi^2} + \frac{1}{\xi}\frac{\partial\hat{\theta}(\xi,s)}{\partial\xi} - Nu^*\hat{\theta}(\xi,s) + \frac{(Q^* + Nu^*\theta_\infty)}{s} = s\hat{\theta}(\xi,s) - \theta(\xi,\tau=0)$$

For clarity, we simply use $\hat{\theta}$ instead of $\hat{\theta}(\xi,s)$ in what follows.

$$\frac{d^2\hat{\theta}}{d\xi^2} + \frac{1}{\xi}\frac{d\hat{\theta}}{d\xi} - Nu^*\hat{\theta} + \frac{(Q^* + Nu^*\theta_\infty)}{s} = s\hat{\theta} - \theta_0$$

$$\frac{d^2\hat{\theta}}{d\xi^2} + \frac{1}{\xi}\frac{d\hat{\theta}}{d\xi} - (Nu^* + s)\hat{\theta} = -[\theta_0 + \frac{(Q^* + Nu^*\theta_\infty)}{s}] \tag{3}$$

B.C. 1:   at $\xi = 0$, $L\left\{\frac{\partial\theta}{\partial\xi}\right\} = \frac{\partial\hat{\theta}}{\partial\xi} = 0$

B.C. 2:   at $\xi = 1$ $\hat{\theta} = \hat{\theta}_f$

The general solution to Eq. (3) is

$$\hat{\theta}(\xi,s) = \frac{[\theta_0 + \frac{(Q^* + Nu^*\theta_\infty)}{s}]}{Nu^* + s} + c_1 J_0(i\xi\sqrt{Nu^* + s}) + c_2 Y_0(i\xi\sqrt{Nu^* + s}) \tag{4}$$

where c_1 and c_2 are constants and J_0 and Y_0 are the Bessel functions of the first and second kinds of zero order respectively. From B.C. 1, for $\hat{\theta}(\xi,s)$ to be finite at $\xi = 0$, $c_2 \equiv 0$ since $Y_0(0)$ approaches minus infinity.

From B.C. 2,

$$c_1 = \frac{\hat{\theta}_f (Nu^* + s) - [\theta_0 + \frac{(Q^* + Nu^* \theta_\infty)}{s}]}{(Nu^* + s) J_0 (i\sqrt{Nu^* + s})}$$

Equation (4) then becomes

$$\hat{\theta}(\xi, s) = \frac{\theta_0}{(Nu^* + s)} + \frac{(Q^* + Nu^* \theta_\infty)}{s(Nu^* + s)}$$

$$+ \left\{ \hat{\theta}_f - \frac{\theta_0}{(Nu^* + s)} - \frac{(Q^* + Nu^* \theta_\infty)}{s(Nu^* + s)} \right\} \frac{J_0(i\xi\sqrt{Nu^* + s})}{J_0(i\sqrt{Nu^* + s})}$$

(5)

Taking the inverse Laplace transform of Eq. (5),

$$\theta(\xi, \tau) = L^{-1} \left\{ \frac{\theta_0}{(Nu^* + s)} \right\} + L^{-1} \left\{ \frac{(Q^* + Nu^* \theta_\infty)}{s(Nu^* + s)} \right\}$$

$$+ L^{-1} \left\{ \hat{\theta}_f \frac{J_0(i\xi\sqrt{Nu^* + s})}{J_0(i\sqrt{Nu^* + s})} \right\} - L^{-1} \left\{ \frac{\theta_0}{(Nu^* + s)} \frac{J_0(i\xi\sqrt{Nu^* + s})}{J_0(i\sqrt{Nu^* + s})} \right\}$$

$$- L^{-1} \left\{ \frac{(Q^* + Nu^* \theta_\infty)}{s(Nu^* + s)} \frac{J_0(i\xi\sqrt{Nu^* + s})}{J_0(i\sqrt{Nu^* + s})} \right\}$$

(6)

The first two inverse Laplace transform terms on the right-hand side of Eq. (6) can be easily obtained.

$$L^{-1} \left\{ \frac{\theta_0}{(Nu^* + s)} \right\} = \theta_0 \exp(-Nu^* \tau)$$

(7)

$$L^{-1} \left\{ \frac{(Q^* + Nu^* \theta_\infty)}{s(Nu^* + s)} \right\} = \frac{(Q^* + Nu^* \theta_\infty)}{Nu^*} \left\{ 1 - \exp(-Nu^* \tau) \right\}$$

(8)

The fourth term on the right-hand side of Eq. (6) can be evaluated as follows. From Stephenson [12],

$$L^{-1} \left\{ \frac{1}{s} \frac{J_0(i\xi\sqrt{s})}{J_0(i\sqrt{s})} \right\} = 1 - 2 \sum_{n=1}^{\infty} \frac{\exp(-\lambda_n^2 \tau)}{\lambda_n} \frac{J_0(\lambda_n \xi)}{J_1(\lambda_n)}$$

(9)

where $\lambda_1, \lambda_2, \lambda_3, \lambda_4, \ldots$ are the positive roots of the equation $J_0(\lambda_n) = 0$. An application of the shift theorem [13] results in

$$L^{-1}\left\{\frac{\theta_0}{(Nu^*+s)}\frac{J_0(i\xi\sqrt{Nu^*+s})}{J_0(i\sqrt{Nu^*+s})}\right\}=\theta_0\exp(-Nu^*\tau)\left\{1-2\sum_{n=1}^{\infty}\frac{\exp(-\lambda_n^2\tau)}{\lambda_n}\frac{J_0(\lambda_n\xi)}{J_1(\lambda_n)}\right\}\qquad(10)$$

The last term on the right-hand side of Eq. (6) can now be obtained using the convolution theorem [13] and Eq. (10).

$$L^{-1}\left\{\frac{(Q^*+Nu^*\theta_\infty)}{s(Nu^*+s)}\frac{J_0(i\xi\sqrt{Nu^*+s})}{J_0(i\sqrt{Nu^*+s})}\right\}=$$

$$(Q^*+Nu^*\theta_\infty)\int_0^\tau\exp(-Nu^*\tau^*)\left\{1-2\sum_{n=1}^{\infty}\frac{\exp(-\lambda_n^2\tau^*)}{\lambda_n}\frac{J_0(\lambda_n\xi)}{J_1(\lambda_n)}\right\}d\tau^*$$

$$L^{-1}\left\{\frac{(Q^*+Nu^*\theta_\infty)}{s(Nu^*+s)}\frac{J_0(i\xi\sqrt{Nu^*+s})}{J_0(i\sqrt{Nu^*+s})}\right\}=$$

$$(Q^*+Nu^*\theta_\infty)\left\{\frac{1-\exp(-Nu^*\tau)}{Nu^*}\right\}-(2Q^*+2Nu^*\theta_\infty)\sum_{n=1}^{\infty}\frac{J_0(\lambda_n\xi)}{\lambda_nJ_1(\lambda_n)}\int_0^\tau\exp(-Nu^*\tau^*)\exp(-\lambda_n^2\tau^*)d\tau^*$$

$$L^{-1}\left\{\frac{(Q^*+Nu^*\theta_\infty)}{s(Nu^*+s)}\frac{J_0(i\xi\sqrt{Nu^*+s})}{J_0(i\sqrt{Nu^*+s})}\right\}=$$

$$(Q^*+Nu^*\theta_\infty)\left\{\frac{1-\exp(-Nu^*\tau)}{Nu^*}\right\}-(2Q^*+2Nu^*\theta_\infty)\sum_{n=1}^{\infty}\frac{J_0(\lambda_n\xi)}{\lambda_nJ_1(\lambda_n)}\left\{\frac{1-\exp[-\tau(Nu^*+\lambda_n^2)]}{Nu^*+\lambda_n^2}\right\}$$

$$(11)$$

The third term on the right-hand side of Eq. (6) can be obtained as follows. First, we re-write this term as

$$L^{-1}\left\{\hat{\theta}_f \frac{J_0(i\xi\sqrt{Nu^*+s})}{J_0(i\sqrt{Nu^*+s})}\right\}$$

$$= L^{-1}\left\{\left[\hat{\theta}_f(Nu^*+s)-\theta_f(\tau=0)+\theta_f(\tau=0)\right]\frac{1}{(Nu^*+s)}\frac{J_0(i\xi\sqrt{Nu^*+s})}{J_0(i\sqrt{Nu^*+s})}\right\}$$

$$= L^{-1}\left\{\left[s\hat{\theta}_f - \theta_f(\tau=0)\right]\frac{1}{(Nu^*+s)}\frac{J_0(i\xi\sqrt{Nu^*+s})}{J_0(i\sqrt{Nu^*+s})}\right\} + L^{-1}\left\{Nu^*\hat{\theta}_f \frac{1}{(Nu^*+s)}\frac{J_0(i\xi\sqrt{Nu^*+s})}{J_0(i\sqrt{Nu^*+s})}\right\}$$

$$+\theta_f(\tau=0)L^{-1}\left\{\frac{1}{(Nu^*+s)}\frac{J_0(i\xi\sqrt{Nu^*+s})}{J_0(i\sqrt{Nu^*+s})}\right\}$$

Then an application of the shift and convolution theorems [13] results in

$$L^{-1}\left\{\hat{\theta}_f \frac{J_0(i\xi\sqrt{Nu^*+s})}{J_0(i\sqrt{Nu^*+s})}\right\} = \int_0^\tau \exp[-Nu^*(\tau-\tau^*)]\left\{1-2\sum_{n=1}^\infty \frac{\exp[-\lambda_n^2(\tau-\tau^*)]}{\lambda_n}\frac{J_0(\lambda_n\xi)}{J_1(\lambda_n)}\right\}\left[\frac{d\theta_f}{d\tau^*}\right]d\tau^*$$

$$+ Nu^*\int_0^\tau \exp[-Nu^*(\tau-\tau^*)]\left\{1-2\sum_{n=1}^\infty \frac{\exp[-\lambda_n^2(\tau-\tau^*)]}{\lambda_n}\frac{J_0(\lambda_n\xi)}{J_1(\lambda_n)}\right\}\theta_f(\tau^*)d\tau^*$$

$$+ \theta_f(\tau=0)\exp[-Nu^*\tau]\left\{1-2\sum_{n=1}^\infty \frac{\exp[-\lambda_n^2\tau]}{\lambda_n}\frac{J_0(\lambda_n\xi)}{J_1(\lambda_n)}\right\}$$

$$(12)$$

Substituting Eqs. (7), (8), (10), (11), and (12) into Eq. (6) and after a few algebraic manipulations, the following dimensionless temperature distribution $\theta(\xi,\tau)$ of the foil is obtained.

$$\theta(\xi,\tau) = \theta_0 \exp(-Nu^*\tau)$$

$$+ \int_0^\tau \exp[-Nu^*(\tau-\tau^*)]\left\{1 - 2\sum_{n=1}^{\infty} \frac{\exp[-\lambda_n^2(\tau-\tau^*)]}{\lambda_n}\frac{J_0(\lambda_n\xi)}{J_1(\lambda_n)}\right\}\left[\frac{d\theta_f}{d\tau^*}\right]d\tau^*$$

$$+ Nu^*\int_0^\tau \exp[-Nu^*(\tau-\tau^*)]\left\{1 - 2\sum_{n=1}^{\infty} \frac{\exp[-\lambda_n^2(\tau-\tau^*)]}{\lambda_n}\frac{J_0(\lambda_n\xi)}{J_1(\lambda_n)}\right\}\theta_f(\tau^*)d\tau^*$$

$$+ \theta_f(\tau=0)\exp(-Nu^*\tau)\left\{1 - 2\sum_{n=1}^{\infty} \frac{\exp(-\lambda_n^2\tau)}{\lambda_n}\frac{J_0(\lambda_n\xi)}{J_1(\lambda_n)}\right\}$$

$$- \theta_0\exp(-Nu^*\tau)\left\{1 - 2\sum_{n=1}^{\infty} \frac{\exp(-\lambda_n^2\tau)}{\lambda_n}\frac{J_0(\lambda_n\xi)}{J_1(\lambda_n)}\right\}$$

$$+ (2Q^* + 2Nu^*\theta_\infty)\sum_{n=1}^{\infty} \frac{J_0(\lambda_n\xi)}{\lambda_n J_1(\lambda_n)}\left\{\frac{1-\exp[-\tau(Nu^*+\lambda_n^2)]}{Nu^*+\lambda_n^2}\right\}$$

(13)

Since the temperature difference between the center of the gage ($\xi = 0$) and the edge (heat sink) of the gage ($\xi = 1$) is directly related to the thin-foil gage operation and measurements, the general expressions for $\theta(\xi=0,\tau)$ and $\theta(\xi=1,\tau)$ with $J_0(0) = 1$ and $J_0(\lambda_n) = 0$ for all λ_n are

$$\theta(\xi=0,\tau) = 2\theta_0\exp(-Nu^*\tau)\sum_{n=1}^{\infty} \frac{\exp(-\lambda_n^2\tau)}{\lambda_n}\frac{1}{J_1(\lambda_n)}$$

$$+ \int_0^\tau \exp[-Nu^*(\tau-\tau^*)]\left\{1 - 2\sum_{n=1}^{\infty} \frac{\exp[-\lambda_n^2(\tau-\tau^*)]}{\lambda_n}\frac{1}{J_1(\lambda_n)}\right\}\left[\frac{d\theta_f}{d\tau^*}\right]d\tau^*$$

$$+ Nu^*\int_0^\tau \exp[-Nu^*(\tau-\tau^*)]\left\{1 - 2\sum_{n=1}^{\infty} \frac{\exp[-\lambda_n^2(\tau-\tau^*)]}{\lambda_n}\frac{1}{J_1(\lambda_n)}\right\}\theta_f(\tau^*)d\tau^*$$

$$+ \theta_f(\tau=0)\exp(-Nu^*\tau)\left\{1 - 2\sum_{n=1}^{\infty} \frac{\exp(-\lambda_n^2\tau)}{\lambda_n}\frac{1}{J_1(\lambda_n)}\right\}$$

$$+ (2Q^* + 2Nu^*\theta_\infty)\sum_{n=1}^{\infty} \frac{1}{\lambda_n J_1(\lambda_n)}\left\{\frac{1-\exp[-\tau(Nu^*+\lambda_n^2)]}{Nu^*+\lambda_n^2}\right\}$$

(14)

$$\theta(\xi=1,\tau)=\int_0^\tau \exp[-Nu^*(\tau-\tau^*)]\left[\frac{d\theta_f}{d\tau^*}\right]d\tau^*$$

$$+ Nu^* \int_0^\tau \exp[-Nu^*(\tau-\tau^*)]\theta_f(\tau^*)d\tau^* + \theta_f(\tau=0)\exp(-Nu^*\tau)$$

(15)

The general expression for $\theta(\xi,\tau)$ can be further simplified if there is no convective heat transfer ($Nu^*=0$), no radiative heat transfer ($Q^*=0$), or pure conduction ($Q^*=0$ and $Nu^*=0$). Since proper operation of thin-foil gages requires constant cooling water temperature to be maintained in the heat sink, a constant boundary condition at the edge of the gage (heat sink), $\theta_f=\theta_0$ = constant, was employed in all previous analytical studies reported in the literature [1-8]. For reference and comparison, the closed-form expressions for $\theta(\xi,\tau)$ and $\theta(\xi=0,\tau)-\theta(\xi=1,\tau)$ under constant boundary condition ($\theta_f=\theta_0$) and various modes of heat transfer are discussed and presented below.

Case 1. No convective heat transfer with $\theta_f = \theta_o$ = constant

If $Nu^*=0$ and $\theta_f(\tau)=\theta_0$ = constant, then Eq. (13) becomes

$$\theta(\xi,\tau)=\theta_0 + 2Q^* \sum_{n=1}^\infty \frac{J_0(\lambda_n\xi)}{\lambda_n^3 J_1(\lambda_n)} - 2Q^* \sum_{n=1}^\infty \frac{J_0(\lambda_n\xi)}{\lambda_n^3 J_1(\lambda_n)}\exp(-\lambda_n^2\tau)$$

(16)

It can be shown [14] that

$$8\sum_{n=1}^\infty \frac{J_0(\lambda_n\xi)}{\lambda_n^3 J_1(\lambda_n)} = 1-\xi^2$$

(17)

Equation (16) can be expressed as

$$\theta(\xi,\tau)=\theta_0 + \frac{Q^*}{4}(1-\xi^2) - 2Q^* \sum_{n=1}^\infty \frac{J_0(\lambda_n\xi)}{\lambda_n^3 J_1(\lambda_n)}\exp(-\lambda_n^2\tau)$$

(18)

Equation (18) is the same equation derived and used by Ash [5] and Keltner and Wildin [7] to study the transient response of thin-foil gages.

$$\theta(\xi=0,\tau)-\theta(\xi=1,\tau)=2Q^* \sum_{n=1}^\infty \frac{1-\exp(-\lambda_n^2\tau)}{\lambda_n^3 J_1(\lambda_n)}$$

(19)

Figure 2 shows the response curve of $\{\theta(\xi = 0, \tau) - \theta(\xi = 1, \tau)\}$ as a function of τ at various $Q*$ and $Nu* = 0$. In obtaining the results in Figure 2, only the sum of the first five terms in the series is needed to achieve convergence.

As $\tau \rightarrow \infty$ (steady state), Eq. (18) becomes

$$\theta(\xi, \tau \rightarrow \infty) = \theta_0 + \frac{Q^*}{4}(1 - \xi^2) \tag{20}$$

The above equation was first derived by Gardon [1]. From Eq. (19),

$$\theta(\xi = 0, \tau \rightarrow \infty) - \theta(\xi = 1, \tau \rightarrow \infty) = 2Q^* \sum_{n=1}^{\infty} \frac{1}{\lambda_n^3 J_1(\lambda_n)}$$

From Eq. (17) and with $\xi = 0$ and $J_0(0) = 1$, $\displaystyle\sum_{n=1}^{\infty} \frac{1}{J_1(\lambda_n)}\left[\frac{1}{\lambda_n^3}\right] = \frac{1}{8}$

$$\theta(\xi = 0, \tau \rightarrow \infty) - \theta(\xi = 1, \tau \rightarrow \infty) = \frac{Q^*}{4} \tag{21}$$

Equation (21) was used by Gardon [1] to obtain thermal radiative heat flux from temperature difference measurements between the foil center and edge and to analyze the performance of the gage.

Case 2. No radiative heat transfer with $\theta_f = \theta_0$ = constant

If $Q^* = 0$ and $\theta_f(\tau) = \theta_0$ = constant, it can be shown that Eq. (13) reduces to

$$\theta(\xi, \tau) = \theta_0 + 2Nu^*(\theta_\infty - \theta_0)\sum_{n=1}^{\infty} \frac{J_0(\lambda_n \xi)}{\lambda_n J_1(\lambda_n)}\left\{\frac{1 - \exp[-\tau(Nu^* + \lambda_n^2)]}{Nu^* + \lambda_n^2}\right\} \tag{22}$$

and

$$\theta(\xi = 0, \tau) - \theta(\xi = 1, \tau) = 2Nu^*(\theta_\infty - \theta_0)\sum_{n=1}^{\infty} \frac{1}{\lambda_n J_1(\lambda_n)}\left\{\frac{1 - \exp[-\tau(Nu^* + \lambda_n^2)]}{Nu^* + \lambda_n^2}\right\} \tag{23}$$

It is interesting to compare our results to Ash's work [5]. The corresponding equation derived by Ash [5] and expressed in terms of the dimensionless variables used in the current work is

$$\theta(\xi = 0, \tau) - \theta(\xi = 1, \tau) = (\theta_\infty - \theta_0)\left\{1 - \frac{1}{I_0(\sqrt{Nu^*})} - 2Nu^*\sum_{n=1}^{\infty} \frac{\exp[-(Nu^* + \lambda_n^2)\tau]}{\lambda_n J_1(\lambda_n)(Nu^* + \lambda_n^2)}\right\} \tag{24}$$

Figure 3 shows the response curves of $\{\theta(\xi = 0, \tau) - \theta(\xi = 1, \tau)\}$ as a function of τ at various $Nu*$ with $Q* = 0$ and $\theta_\infty = 2$ calculated using Eq. (23) from our work and Eq. (24) from Ash (1969). Since the results obtained from Eq. (23) is identical to those from Eq. (24), as demonstrated in Figure 3, we obtain the following identity.

$$\left\{ 1 - \frac{1}{I_0(\sqrt{Nu^*})} \right\} = 2Nu^* \sum_{n=1}^{\infty} \frac{1}{\lambda_n J_1(\lambda_n)(Nu^* + \lambda_n^2)} \tag{25}$$

As $\tau \to \infty$ (steady state), Eq. (23) becomes

$$\theta(\xi = 0, \tau \to \infty) - \theta(\xi = 1, \tau \to \infty) = 2Nu^*(\theta_\infty - \theta_0) \sum_{n=1}^{\infty} \frac{1}{\lambda_n J_1(\lambda_n)(Nu^* + \lambda_n^2)} \tag{26}$$

It is worth pointing out that the corresponding equation derived by Kuo and Kulkarin [9] and expressed in terms of the dimensionless variables used in the current work is

$$\theta_{\xi=0} - \theta_{\xi=1} = (\theta_\infty - \theta_0)[1 - \frac{1}{I_0(\sqrt{Nu^*})}] \tag{27}$$

Based on Eq. (25), Eq. (26) is identical to Eq. (27), which can also be deduced from Eq. (24) when $\tau \to \infty$.

Case 3. Pure heat conduction with $\theta_f = \theta_0$ = constant

In this case, $Q^* = 0$, $Nu^* = 0$, and $\theta_f = \theta_0$, then Eq. (13) trivially becomes

$$\theta(\xi, \tau) = \theta_0 \tag{28}$$

Case 4. Radiative and convective heat transfer with $\theta_f = \theta_0$ = constant

In this case, $Q^* \neq 0$, $Nu^* \neq 0$, and $\theta_f(\tau) = \theta_0$ = constant. Eq. (13) becomes

$$\theta(\xi, \tau) = \theta_0 \exp(-Nu^* \tau)$$

$$+ \theta_0 Nu^* \int_0^\tau \exp[-Nu^*(\tau - \tau^*)] \left\{ 1 - 2 \sum_{n=1}^\infty \frac{\exp[-\lambda_n^2(\tau - \tau^*)]}{\lambda_n} \frac{J_0(\lambda_n \xi)}{J_1(\lambda_n)} \right\} d\tau^*$$

$$+ \theta_0 \exp(-Nu^* \tau) \left\{ 1 - 2 \sum_{n=1}^\infty \frac{\exp(-\lambda_n^2 \tau)}{\lambda_n} \frac{J_0(\lambda_n \xi)}{J_1(\lambda_n)} \right\}$$

$$- \theta_0 \exp(-Nu^* \tau) \left\{ 1 - 2 \sum_{n=1}^\infty \frac{\exp(-\lambda_n^2 \tau)}{\lambda_n} \frac{J_0(\lambda_n \xi)}{J_1(\lambda_n)} \right\}$$

$$+ (2Q^* + 2Nu^* \theta_\infty) \sum_{n=1}^\infty \frac{J_0(\lambda_n \xi)}{\lambda_n J_1(\lambda_n)} \left\{ \frac{1 - \exp[-\tau(Nu^* + \lambda_n^2)]}{Nu^* + \lambda_n^2} \right\}$$

$$(29)$$

and

$$\theta(\xi = 0, \tau) - \theta(\xi = 1, \tau) = 2[Q^* + Nu^*(\theta_\infty - \theta_0)] \sum_{n=1}^\infty \frac{1}{\lambda_n J_1(\lambda_n)} \left\{ \frac{1 - \exp[-\tau(Nu^* + \lambda_n^2)]}{(Nu^* + \lambda_n^2)} \right\} \quad (30)$$

Figure 4 shows the response curve of $\{\theta(\xi = 0, \tau) - \theta(\xi = 1, \tau)\}$ as a function of τ at various $Nu*$ and $Q* = 2$ and $\theta_\infty = 2$. Within the range of Nu^* used in this study, the effect of convective heat transfer on the gage measurement is not significant.

As $\tau \to \infty$ (steady state), Eq. (30) becomes

$$\theta(\xi = 0, \tau \to \infty) - \theta(\xi = 1, \tau \to \infty) = 2[Q^* + Nu^*(\theta_\infty - \theta_0)] \sum_{n=1}^\infty \frac{1}{\lambda_n J_1(\lambda_n)(Nu^* + \lambda_n^2)} \quad (31)$$

The corresponding equation derived by Kuo and Kulkarni [9] and expressed in terms of the dimensionless variables used in the current work is

$$\theta_{\xi=0} - \theta_{\xi=1} = \left[\theta_0 - (\frac{Q^*}{Nu^*} + \theta_\infty) \right] \left[\frac{1}{I_0(\sqrt{Nu^*})} - 1 \right] \quad (32)$$

Again, using the identity shown in Eq. (25), it can be easily shown that the steady-state temperature difference at the foil center and edge calculated using Eq. (31) and that of Kuo and Kulkarni [9], Eq. (32), are identical.

Figure 5 shows the steady-state dimensionless temperature difference at the foil center and edge calculated using Eq. (31) as a function of $Q*$ at various Nu^* and $\theta_\infty = 2$.

Remarks on Calibration

Gardon gages are normally calibrated under steady-state conditions using prescribed incident radiative fluxes from a radiative heat source. If the gage is used in a purely convective or a mixed convective and radiative environment, correction to the calibration is needed. The correction can be obtained by equating the calibrated response of the purely radiative case to the measured response of the purely convective or the mixed cases.

Equating Eq. (21) to Eq. (26) and simplifying,

$$\frac{\left[Nu^*(\theta_\infty - \theta_0)\right]_{measured}}{\left[Q^*\right]_{calibrated}} = \frac{1}{8} \frac{1}{\displaystyle\sum_{n=1}^{\infty} \frac{1}{\lambda_n J_1(\lambda_n)(Nu^* + \lambda_n^2)}} \tag{33}$$

Equating Eq. (21) to Eq. (31) and simplifying,

$$\frac{\left[Q^* + Nu^*(\theta_\infty - \theta_0)\right]_{measured}}{\left[Q^*\right]_{calibrated}} = \frac{1}{8} \frac{1}{\displaystyle\sum_{n=1}^{\infty} \frac{1}{\lambda_n J_1(\lambda_n)(Nu^* + \lambda_n^2)}} \tag{34}$$

Similar to the results from Kuo and Kulkarni [9], the correction factors for the purely convective case, Eq. (33), and mixed convective and radiative case, Eq. (34), have the same form. Equation (34) is also analogous to the results given in Kuo and Kulkarni [9] and Fu et al. [10].

Conclusions

An expanded analysis of a thin-foil gage, which includes the transient effects, convective heat transfer, and an arbitrary time-varying boundary condition at the edge of the foil, has been performed. The general closed-form solution is obtained using Laplace transform. Specialized solutions under constant temperature at the edge of the foil and constant thermal radiative heat flux are provided under various modes of heat transfer. Steady-state solutions are also obtained as limiting cases. The transient and steady-steady solutions reduced to and matched the results reported in the literature under the less generalized conditions.

Nomenclature

c_p	heat capacity of foil
$f(t)$	heat sink temperature as a function of t
h	convective heat transfer coefficient
H	foil thickness
i	imaginary number, $\sqrt{-1}$
I_0	modified Bessel function of the first kind of zero order
J_0	Bessel function of the first kind of zero order
J_1	Bessel function of the first kind of first order
k	thermal conductivity of foil
k_f	thermal conductivity of fluid
L	Laplace transform operator
L^{-1}	inverse Laplace transform operator
Nu	Nusselt number ($Nu = hR / k_f$)
Nu^*	$= \kappa \delta Nu$
q_i	radiative heat flux
Q^*	$= q_i R^2 / (kHT_0)$
r	radial direction
R	radius of foil
s	variable in Laplace transform domain
t	time
T	absolute temperature
T_0	initial foil temperature
T_∞	temperature of fluid flowing over the foil
Y_0	Bessel function of the second kind of zero order
α	thermal diffusivity of foil, $= k / (\rho c_p)$
δ	$= R / H$
κ	$= k_f / k$

|	
λ_n	zeros of Bessel function of the first kind of zero order
θ	$= T/T_0$
θ_f	$= f(\tau)/T_0$
θ_0	$= T_0/T_0 = 1$
$\hat{\theta}$	$= L\{\theta\}$, Laplace transform of θ
$\hat{\theta}_f$	$= L\{\theta_f\}$, Laplace transform of θ_f
ρ	density of foil
τ	$= \alpha t/R^2$
τ^*	integration dummy variable
ξ	$= r/R$

References

[1] R. Gardon, An Instrument for direct measurement of intense thermal radiation, Review of Scientific Instruments 24 (1953) 366-370.

[2] Fire Tests – Full-Scale Room Test for Surface Products, ISO 9705, International Organization for Standardization, Geneva, Switzerland, 1993.

[3] E. Guillot, I. Alxneit, J. Ballestrin, J.L. Sans, C. Willsh, Comparison of 3 heat flux gauges and a water calorimeter for concentrated solar irradiance measurement Energy Procedia 49 (2014) 2090 – 2099.

[4] E.W. Marlone, Design and calibration of thin-foil heat flux sensors, ISA Transactions 7 (1968) 175-180.

[5] R.L. Ash, Response characteristics of thin foil heat flux sensors, AIAA Journal 7 (1969) 2332-2335.

[6] R.H. Kirchoff, Response of finite-thickness Gardon heat flux sensors, ASME Journal of Heat Transfer 94 (1972) 244-245.

[7] N.R. Keltner, M.W. Wildin, Transient response of circular foil heat flux gages to radiative fluxes, Review of Scientific Instruments 46 (1975) 1161-1166.

[8] G.J. Borell, T.E. Diller, A convection calibration method for local heat flux gages, ASME Journal of Heat Transfer 106 (1987) 83-89.

[9] C.H. Kuo, A.K. Kulkarni, Analysis of heat flux measurement by circular foil gages in a mixed convection/radiation environment, ASME Journal of Heat Transfer 113 (1991) 1037-1040.

[10] T. Fu, A. Zong, Y. Zhang, H.S. Wang, A method to measure heat flux in convection using Gardon gauge, Applied Thermal Engineering 108 (2016) 1357-1361.

[11] T. Fu, A. Zong, J. Tian, C. Xin, Gardon gauge measurements of fast heat flux transients, Applied Thermal Engineering 100 (2016) 501–507.

[12] G. Stephenson, An Introduction to Partial Differential Equations for Science Students, second ed., Longman, London, 1970, p. 113.

[13] E. Kreyszig, Advanced Engineering Mathematics, fifth ed., John Wiley & Sons, New York, 1983, Chapter 5.

[14] R.B. Bird, W.E. Stewart, E.N. Lightfoot, Transport Phenomena, John Wiley & Sons, New York, 1960, p. 129.
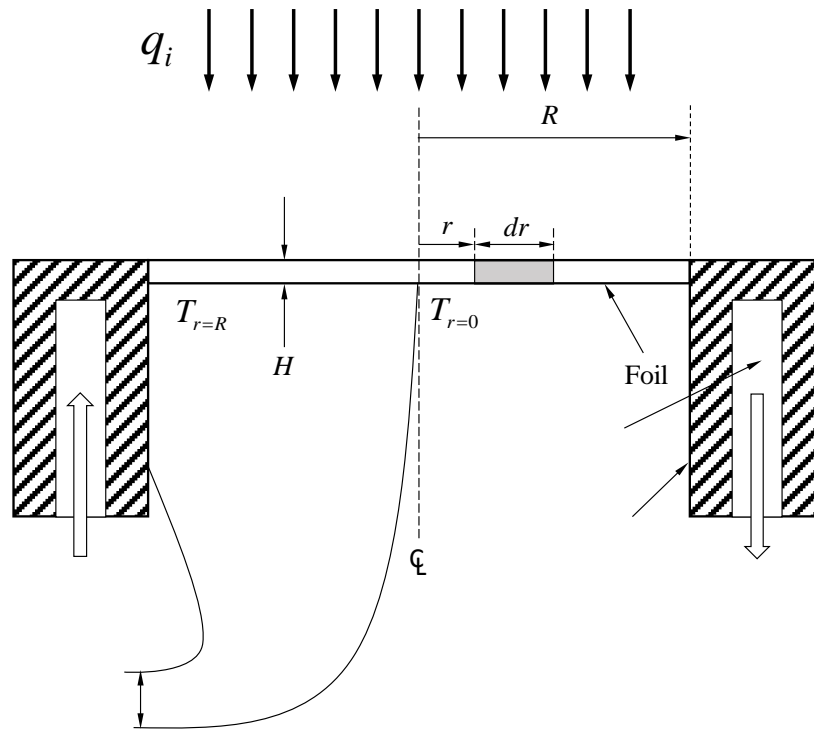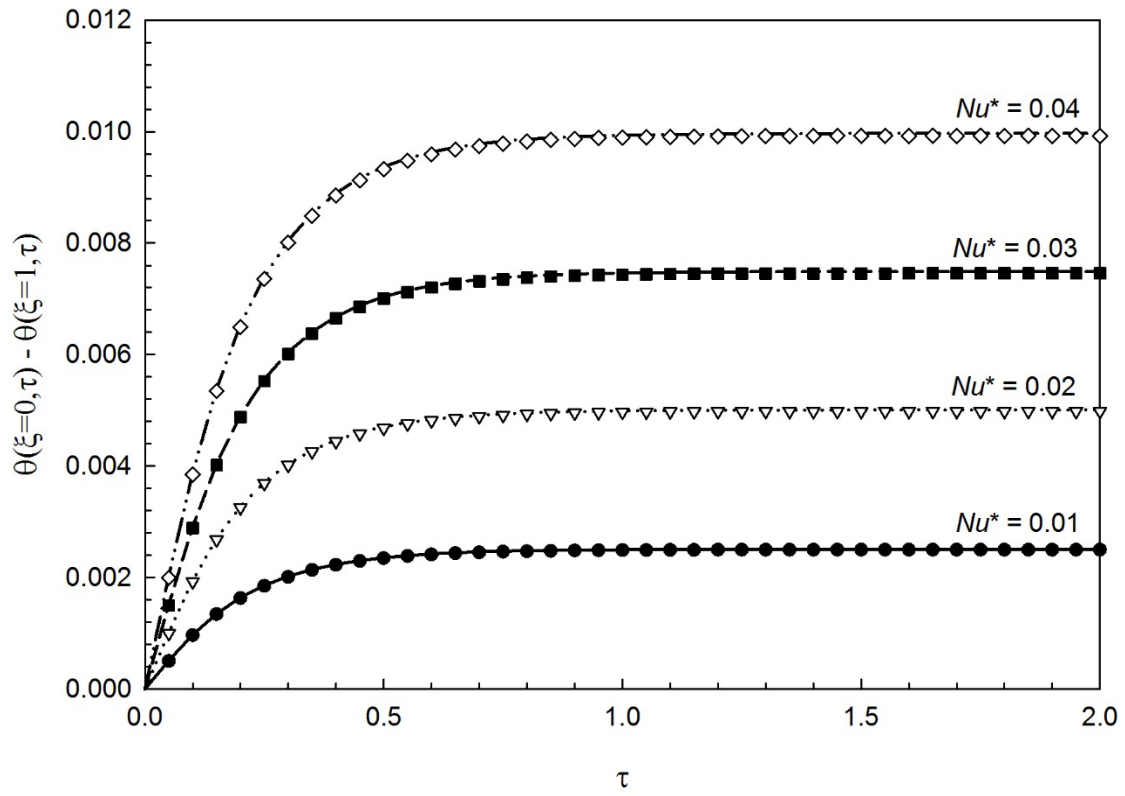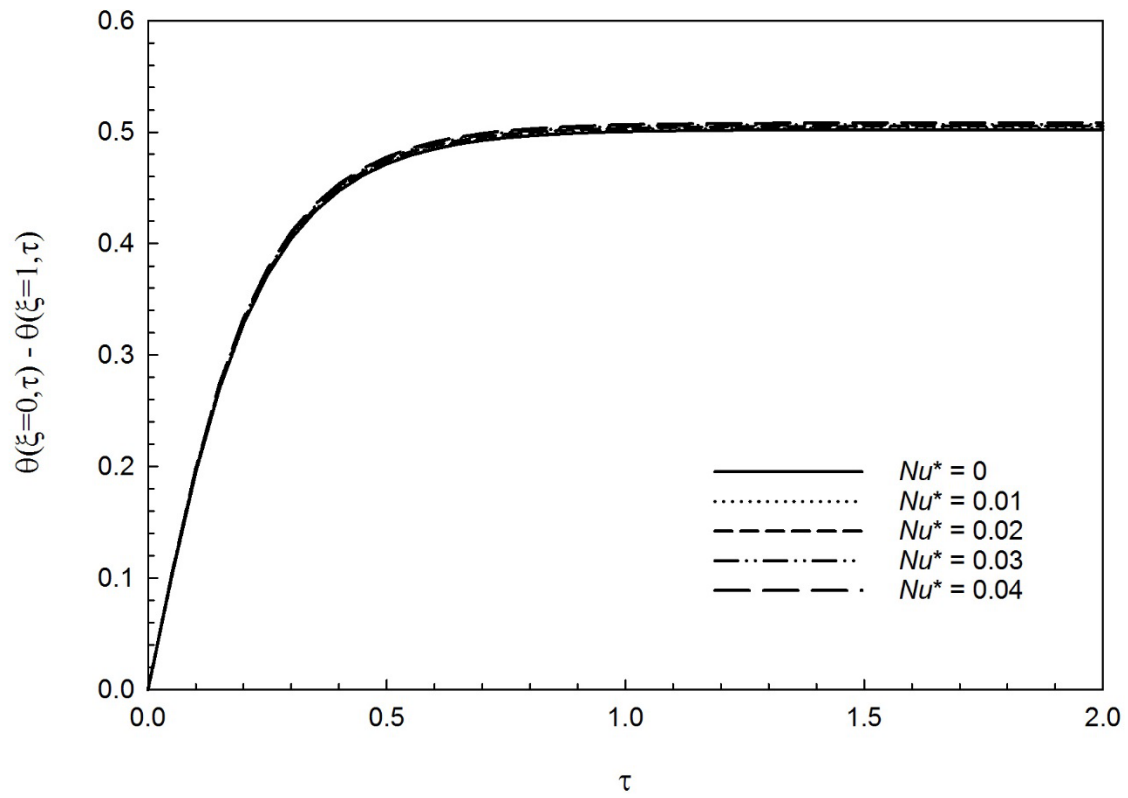
Figure 1. Cross section of a thin-foil gage.
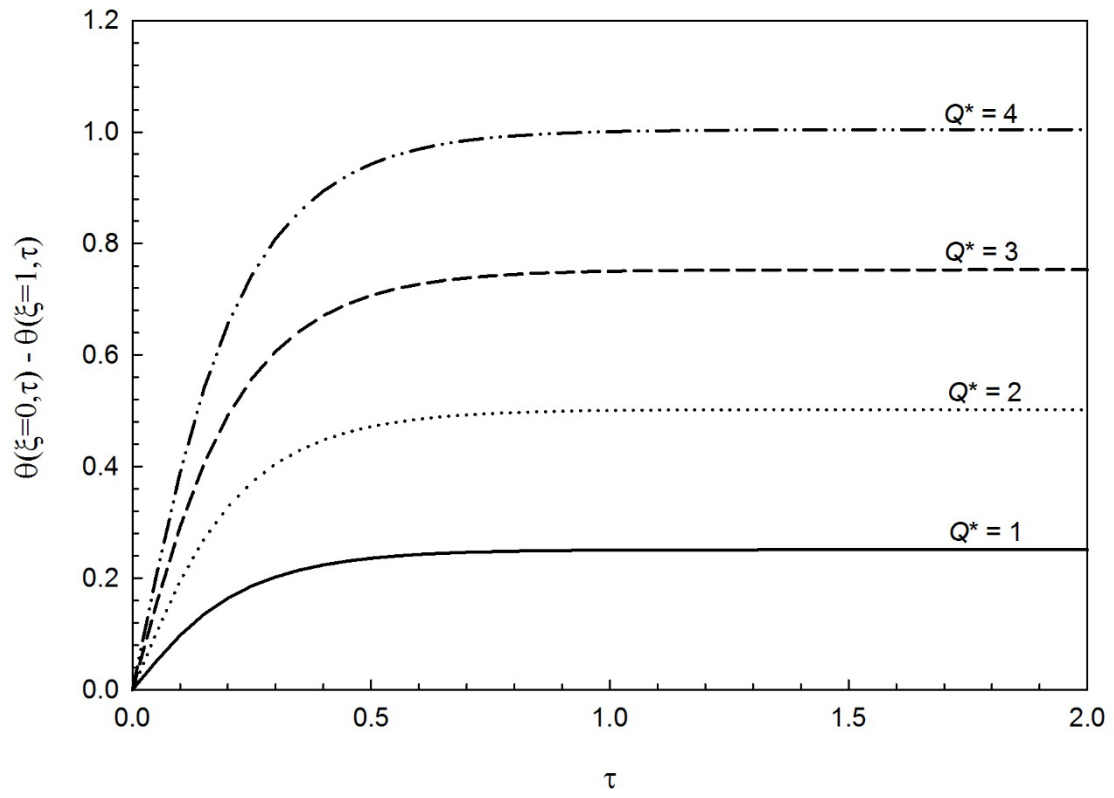
Figure 2. Response curve showing dimensionless temperature difference between the center and edge of gage with no convective heat transfer ($Nu^* = 0$) at various Q^*.

Figure 3. Comparison of response curves showing dimensionless temperature difference between the center and edge of gage with no thermal radiative heat transfer ($Q^* = 0$) at various Nu^* and $\theta_\infty = 2$ from current work (lines) with that from Ash (1969) (symbols).

Figure 4. Response curve showing dimensionless temperature difference between the center and edge of gage with $Q^* = 2$ and $\theta_\infty = 2$ at various Nu^*.
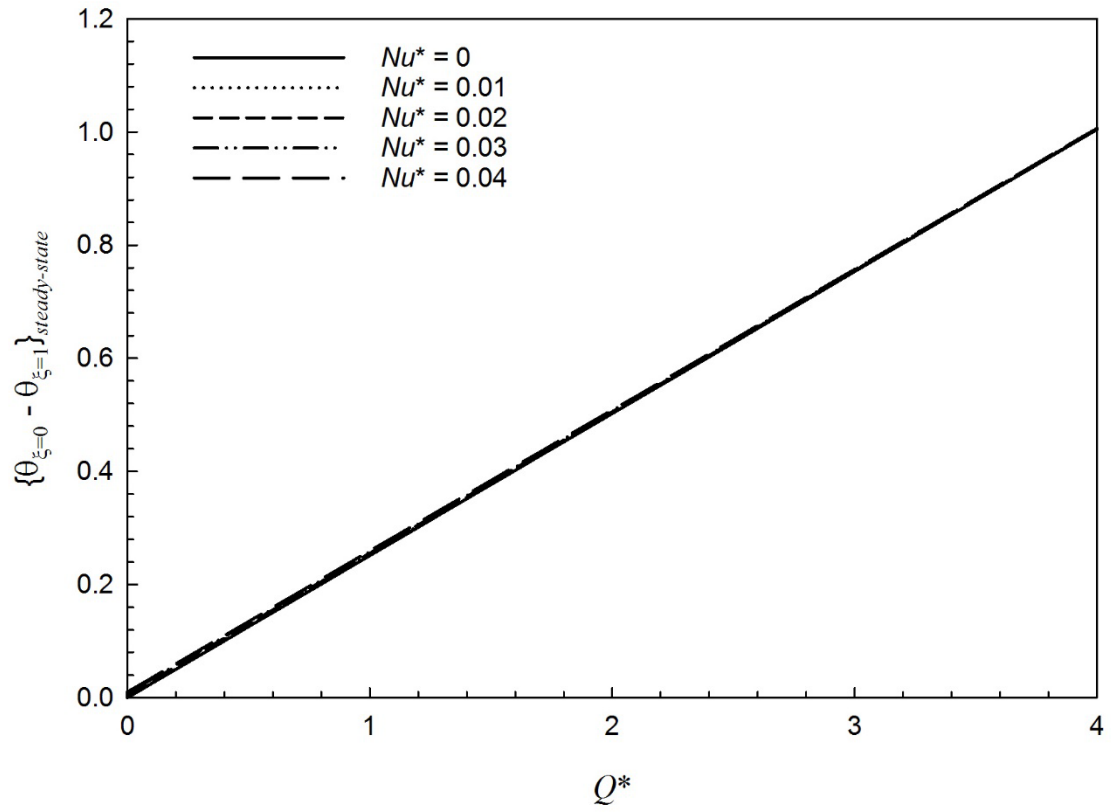
Figure 5. Steady state dimensionless temperature difference between the center and edge of gage as a function of Q^* at various Nu^* with $\theta_\infty = 2$.